

# Scale invariance and the Diophantine approximation in the Bloch vector of the thermal multi-photon Jaynes-Cummings model

**Hiroo Azuma**

Global Research Center for Quantum Information Science, National Institute of Informatics, 2-1-2 Hitotsubashi, Chiyoda-ku, Tokyo 101-8430, Japan

E-mail: zuma@nii.ac.jp

**Abstract.** In this paper, we study the time evolution of the Bloch vector of the thermal multi-photon Jaynes-Cummings model (JCM) and discuss the following two facts. First, we consider a plot that consists of points of a trajectory of the Bloch vector of the multi-photon JCM for a discrete-time sequence with a constant time interval. We show that this plot is invariant under a scale transformation of the finite but not zero interval of the time. Second, we numerically evaluate values of the time when the absolute value of the  $z$ -component of the Bloch vector is nearly equal to zero. We demonstrate that some values of the time can be derived with denominators of fractions of the Diophantine approximation for irrational numbers. The origin of those phenomena is that the components of the Bloch vector for thermal multi-photon JCM cannot be described with the Fourier series.

*Keywords:* multi-photon Jaynes-Cummings model, thermal effect, Bloch vector, scale invariance, Diophantine approximation

## 1. Introduction

For the past years, we have witnessed rapid progress in the technologies of quantum computation. To realize practical quantum computation, we need to implement quantum bits (qubits) and quantum gates that generate entanglement between two qubits. Possible candidates for the construction of qubits are superconducting Josephson-junction devices [1, 2], linear trapped ions [3, 4], quantum dots [5, 6], photons working in linear optical circuits [7, 8], and so on. In association with the developments of manufacturing technologies of the qubits, theoretical and experimental aspects of quantum optics draw the attention of many researchers in the field of quantum information science because quantum optics has a wide range of applications in quantum computation, information, and cryptography.

The Jaynes-Cummings model (JCM) is a typical system of quantum optics. Because the JCM gives us a simple situation where the raising and lowering operators of an atom

couple with the single annihilation and creation operators of photons, respectively, it has been studied eagerly since the 1980s [9, 10]. Because the JCM gives us a fully quantum and solvable system, it is often used as a convenient test bed for studying the quantum properties of the atom and photons.

A multiple-photon JCM is a natural extension of the JCM. The multi-photon JCM has an interaction Hamiltonian which allows couplings of raising and lowering operators of the atom and annihilation and creation operators of  $l$  photons, respectively, for  $l = 2, 3, \dots$ . Implementation of the two-photon JCM has been discussed for a single atom inside an optical cavity [11, 12], and superconducting circuits [13]. We can construct the two-photon JCM from the two-photon quantum Rabi model (QRM) by neglecting counter-rotating terms. A scheme for realizing two-photon QRM with trapped ions was proposed [14]. The two-mode multi-photon JCM has been recently investigated for examining quantum properties of noisy cases and deriving analytical solutions of ideal noiseless cases [15, 16].

In this paper, we study the time evolution of the Bloch vector of the  $l$ -photon JCM for  $l = 2, 3, 4$  where the photons are in contact with a thermal reservoir. We show the following two facts. The first one is as follows. We plot a trajectory of the time evolution of the Bloch vector  $\mathbf{S}(t)$  as a discrete sequence of points on the  $xz$ -plane  $\{(S_x(t), S_z(t)) : t = n\Delta t, n = 0, 1, 2, \dots, N\}$  for large  $N$ . Then, the obtained graph is invariant under a scale transformation of  $\Delta t \rightarrow s\Delta t$  where  $s$  is an arbitrary real but not transcendental number and  $\pi < s\Delta t \pmod{2\pi}$  with  $\pi < \Delta t \pmod{2\pi}$ . The second one is as follows. We numerically evaluate values of the time when the absolute value of the  $z$ -component of the Bloch vector is nearly equal to zero, that is to say,  $|S_z(t)| < \epsilon$  for a small positive number  $\epsilon (\ll 1)$ . Then, we can derive some of those time values by deriving denominators of fractions of the Diophantine approximations of irrational numbers. These two facts were already shown for the original JCM in [17]. The new results of this paper are that the above two facts hold for the multi-photon JCM, as well. Hence, this paper is a sequel to [17].

The origin that causes the above two phenomena is that the components of the Bloch vector cannot be described with the Fourier series. We derive the closed mathematical forms of the components of the Bloch vector which include terms of  $\cos(\sqrt{nt})$  and  $\sin(\sqrt{nt})$  where  $n$  denotes integers for summations in cases with the finite but not zero temperature. (Strictly speaking,  $n$  represents the number of thermal photons in the Bose-Einstein distribution at finite temperature.) Thus, our results obtained in this paper essentially depend on thermal effects.

This paper is organized as follows. In Sec. 2, we derive closed mathematical expressions of the Bloch vector of the multi-photon JCMs. In Sec. 3, we draw graphs of discrete plots of the time evolution of the Bloch vector and show that those graphs are invariant under scale transformations of the time variable. In Sec. 4, we numerically calculate values of the time when the absolute value of the  $z$ -component of the Bloch vector is nearly equal to zero and plot  $(\beta, S_x(t))$  for the time  $t$  such that  $|S_z(t)| < \epsilon$ . Then, we show that those values of  $t$  can be derived by the Diophantine approximations

for an example of the two-photon JCM. In Sec. 5, we give brief discussion. In Appendix A, we give details of computation of the time  $t$  such that  $|S_z(t)| < \epsilon$  for the  $l$ -photon JCMs with  $l = 1, 3$ , and 4 by the Diophantine approximations.

## 2. The Bloch vector of the multi-photon JCM

The Hamiltonian of the original and the multi-photon JCMs is given by

$$H = \frac{\omega_0}{2}\sigma_z + \omega a^\dagger a + g[\sigma_+ a^l + \sigma_-(a^\dagger)^l] \quad \text{for } l = 1, 2, 3, \dots, \quad (1)$$

where  $\sigma_z$ ,  $\sigma_+$ , and  $\sigma_-$  are the Pauli  $z$ -operator, the raising and lowering operators of the atom, and  $a$  and  $a^\dagger$  are annihilation and creation operators of photons, respectively. We put  $\hbar = 1$ , and  $\omega_0$  and  $\omega$  are angular frequencies of the atom and photons, respectively. Here, we pay attention to the fact that we must fix  $l$  at a certain integer for advancing concrete calculations.

Now, we divide  $H$  as follows:

$$\begin{aligned} H &= C_1 + C_2, \\ C_1 &= \omega[(l/2)\sigma_z + a^\dagger a], \\ C_2 &= -(\Delta\omega/2)\sigma_z + g[\sigma_+ a^l + \sigma_-(a^\dagger)^l], \end{aligned} \quad (2)$$

$$\Delta\omega = -\omega_o + l\omega. \quad (3)$$

Then, we obtain  $[C_1, C_2] = 0$  and we can adopt the interaction picture for describing the wave function. Thus, we write the state of the system as

$$|\Psi_I(t)\rangle = U(t)|\Psi_I(0)\rangle, \quad (4)$$

$$\begin{aligned} U(t) &= \exp(-iC_2 t) \\ &= \begin{pmatrix} u_{00} & u_{01} \\ u_{10} & u_{11} \end{pmatrix}, \end{aligned} \quad (5)$$

where we represent the orthonormal basis of the atom as two-component vectors,

$$|0\rangle_A = \begin{pmatrix} 1 \\ 0 \end{pmatrix}, \quad |1\rangle_A = \begin{pmatrix} 0 \\ 1 \end{pmatrix}. \quad (6)$$

Explicit forms of matrix elements of  $U(t)$  are given by the forms,

$$\begin{aligned} u_{00} &= \cos(\sqrt{D}t) + i\frac{\Delta\omega}{2}\frac{\sin(\sqrt{D}t)}{\sqrt{D}}, \\ u_{01} &= -ig\frac{\sin(\sqrt{D}t)}{\sqrt{D}}a^l, \\ u_{10} &= -ig\frac{\sin(\sqrt{D'}t)}{\sqrt{D'}}(a^\dagger)^l, \\ u_{11} &= \cos(\sqrt{D'}t) - i\frac{\Delta\omega}{2}\frac{\sin(\sqrt{D'}t)}{\sqrt{D'}}, \end{aligned} \quad (7)$$

$$\begin{aligned} D &= (\Delta\omega/2)^2 + g^2 a^l (a^\dagger)^l, \\ D' &= (\Delta\omega/2)^2 + g^2 (a^\dagger)^l a^l. \end{aligned} \quad (8)$$

We set the initial state of the atom and photons as  $\rho_{\text{AP}}(0) = \rho_{\text{A}}(0) \otimes \rho_{\text{P}}$ . Thus,  $\rho_{\text{AP}}(0)$  is a disentangled state between the atom and photons. We define matrix elements of  $\rho_{\text{A}}(0)$  as

$$\rho_{\text{A}}(0) = \sum_{i,j \in \{0,1\}} \rho_{\text{A},ij}(0) |i\rangle_{\text{AA}} \langle j|. \quad (9)$$

We assume that the density operator  $\rho_{\text{P}}$  is given by the Bose-Einstein distribution, so that

$$\rho_{\text{P}} = (1 - e^{-\beta\omega}) \exp(-\beta\omega a^\dagger a), \quad (10)$$

and  $\beta = 1/k_{\text{B}}T$ , where  $T$  and  $k_{\text{B}}$  denote the temperature and the Boltzman constant, respectively.

The time evolution of the state of the atom is given by

$$\begin{aligned} \rho_{\text{A}}(t) &= \text{Tr}_{\text{P}}[U(t)\rho_{\text{AP}}(0)U^\dagger(t)] \\ &= \sum_{k,m \in \{0,1\}} \rho_{\text{A},km}(t) |k\rangle_{\text{AA}} \langle m|, \end{aligned} \quad (11)$$

where

$$\rho_{\text{A},km}(t) = \sum_{i,j \in \{0,1\}} \rho_{\text{A},ij}(0) A_{ij,km}(t) \quad \text{for } k, m \in \{0, 1\}, \quad (12)$$

$$A_{ij,km}(t) = {}_{\text{A}}\langle k | \text{Tr}_{\text{P}}[U(t)(|i\rangle_{\text{AA}} \langle j| \otimes \rho_{\text{P}})U^\dagger(t)] |m\rangle_{\text{A}}. \quad (13)$$

The matrix elements of  $\rho_{\text{A}}(t)$  satisfy the relationships,  $\rho_{\text{A},10}(t) = \rho_{\text{A},01}(t)^*$  and  $\rho_{\text{A},11}(t) = 1 - \rho_{\text{A},00}(t)$ . Thus, from now on, what we have to do is computing only  $\rho_{\text{A},00}(t)$  and  $\rho_{\text{A},01}(t)$ . We can derive the matrix elements  $A_{ij,km}(t)$  in the forms,

$$\begin{aligned} A_{00,00}(t) &= (1 - e^{-\beta\omega}) \sum_{n=0}^{\infty} e^{-n\beta\omega} \left[ \cos^2(\sqrt{D_n}t) + \left(\frac{\Delta\omega}{2}\right)^2 \frac{\sin^2(\sqrt{D_n}t)}{D_n} \right], \\ A_{11,00}(t) &= g^2 \sum_{n=0}^{\infty} \frac{\sin^2(\sqrt{D_n}t)}{D_n} (1 - e^{-\beta\omega}) \prod_{k=1}^l (n+k) e^{-(n+l)\beta\omega}, \\ A_{01,01}(t) &= \sum_{n=0}^{\infty} \left[ \cos(\sqrt{D_n}t) + i \frac{\Delta\omega}{2} \frac{\sin(\sqrt{D_n}t)}{\sqrt{D_n}} \right] \\ &\quad \times \left[ \cos(\sqrt{D'_n}t) + i \frac{\Delta\omega}{2} \frac{\sin(\sqrt{D'_n}t)}{\sqrt{D'_n}} \right] (1 - e^{-\beta\omega}) e^{-n\beta\omega}, \end{aligned} \quad (14)$$

and  $A_{01,00}(t) = A_{10,00}(t) = A_{00,01}(t) = A_{10,01}(t) = A_{11,01}(t) = 0$ . Then, we obtain

$$\begin{aligned} \rho_{\text{A},00}(t) &= \rho_{\text{A},00}(0) A_{00,00}(t) + \rho_{\text{A},11}(0) A_{11,00}(t), \\ \rho_{\text{A},01}(t) &= \rho_{\text{A},01}(0) A_{01,01}(t). \end{aligned} \quad (15)$$

Introducing the Bloch vector  $\mathbf{S}(t) = (S_x(t), S_y(t), S_z(t))$  as

$$\rho_{\text{A}}(t) = \frac{1}{2} [\mathbf{I} + \mathbf{S}(t) \cdot \boldsymbol{\sigma}], \quad (16)$$

we obtain

$$\mathbf{S}(t) = \begin{pmatrix} L^{(1)}(t) & L^{(2)}(t) & 0 \\ -L^{(2)}(t) & L^{(1)}(t) & 0 \\ 0 & 0 & L^{(3)}(t) \end{pmatrix} \mathbf{S}(0) + \begin{pmatrix} 0 \\ 0 \\ L^{(4)}(t) \end{pmatrix}, \quad (17)$$

$$\begin{aligned} L^{(1)}(t) &= \text{Re}[A_{01,01}(t)], \\ L^{(2)}(t) &= \text{Im}[A_{01,01}(t)], \\ L^{(3)}(t) &= A_{00,00}(t) - A_{11,00}(t), \\ L^{(4)}(t) &= A_{00,00}(t) + A_{11,00}(t) - 1. \end{aligned} \quad (18)$$

Now, we consider a special case where  $\Delta\omega = 0$ . This implies that we can adjust  $\omega_0$  and let it satisfy a relationship  $\omega_0 = l\omega$ . Then,  $A_{01,01}(t)$  becomes a real number and we obtain  $L^{(2)}(t) = 0$ . Moreover, setting the initial state of the atom at  $\rho_A(0) = |\psi\rangle_{AA}\langle\psi|$  and  $|\psi\rangle_A = (1/\sqrt{2})(|0\rangle_A + |1\rangle_A)$ , we can put the initial Bloch vector as  $\mathbf{S}(0) = (1, 0, 0)^T$ . Finally, we attain

$$\mathbf{S}(t) = \begin{pmatrix} L^{(1)}(t) \\ 0 \\ L^{(4)}(t) \end{pmatrix}. \quad (19)$$

Thus, in this circumstance, we only need to consider the Bloch vector that lies on the  $xz$ -plane.

### 3. Discrete plots of the time evolution of the Bloch vector

In this section, we consider the following graph of  $\mathbf{S}(t)$  given by Eqs. (18) and (19). We plot  $\mathbf{S}(t)$  at a constant time interval  $\Delta t$  on the  $xz$ -plane, that is to say, values of the time variable are given by a sequence of  $t_n = n\Delta t$  for  $n = 0, 1, 2, \dots, N$  with large  $N$ . In Figs. 1, 2, 3, and 4, we plot the discrete trajectory of  $\mathbf{S}(t_n)$  on the  $xz$ -plane.

The graphs of Figs. 1, 2, 3, and 4 are invariant under a scale transformation  $\Delta t \rightarrow s\Delta t$  where  $s$  is an arbitrary real but not a transcendental number and  $\pi < s\Delta t \pmod{2\pi}$  with  $\pi < \Delta t \pmod{2\pi}$ . Here, we explain the reason why the above statement holds. First, we consider a set of  $N$  numbers,  $\mathcal{S}_N = \{x_j : 0 \leq x_j < 2\pi, j \in \{0, 1, \dots, N\}\}$ . The necessary and sufficient condition that the sequence  $(x_0, x_1, \dots, x_N)$  is uniformly distributed in the range of  $[0, 2\pi)$  under the limit of  $N \rightarrow +\infty$  is given as follows [18, 19, 20, 21]:

$$\lim_{N \rightarrow +\infty} \frac{1}{N+1} \sum_{j=0}^N \exp(imx_j) = 0 \quad \forall m \in \{\pm 1, \pm 2, \dots\}. \quad (20)$$

Here, we let  $\mathcal{S}_N = \{x_n = n\Delta t \pmod{2\pi} : n \in \{0, 1, \dots, N\}\}$ . Then, we obtain

$$\lim_{N \rightarrow +\infty} \frac{1}{N+1} \sum_{n=0}^N \exp(imx_n) = \lim_{n \rightarrow +\infty} \frac{1}{N+1} \frac{1 - e^{im(N+1)\Delta t}}{1 - e^{im\Delta t}}. \quad (21)$$

Thus, if  $m\Delta t \pmod{2\pi} \neq 0 \quad \forall m \in \{\pm 1, \pm 2, \dots\}$ , the right-hand side of Eq. (21) is equal to zero. Hence, if  $\Delta t$  is real, positive, but not transcendental number,

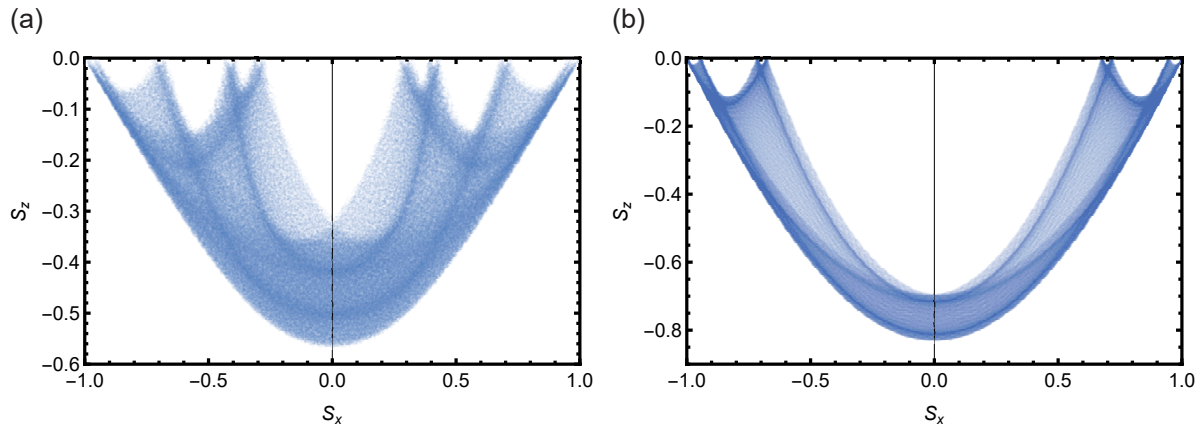


**Figure 1.** Graphs that consist of dots of  $\mathcal{S}(t)$  given by Eqs. (18) and (19) for the original JCM ( $l = 1$ ). The dots are plotted at the constant time interval  $\Delta t = 4$  for  $\omega = 1$ ,  $g = 1$ , and  $\Delta\omega = 0$ . The total number of the dots is given by  $N = 400001$ . We set these parameters in Figs. 2, 3, and 4, as well. (a)  $\beta = 0.9$ . (b)  $\beta = 1.8$ .

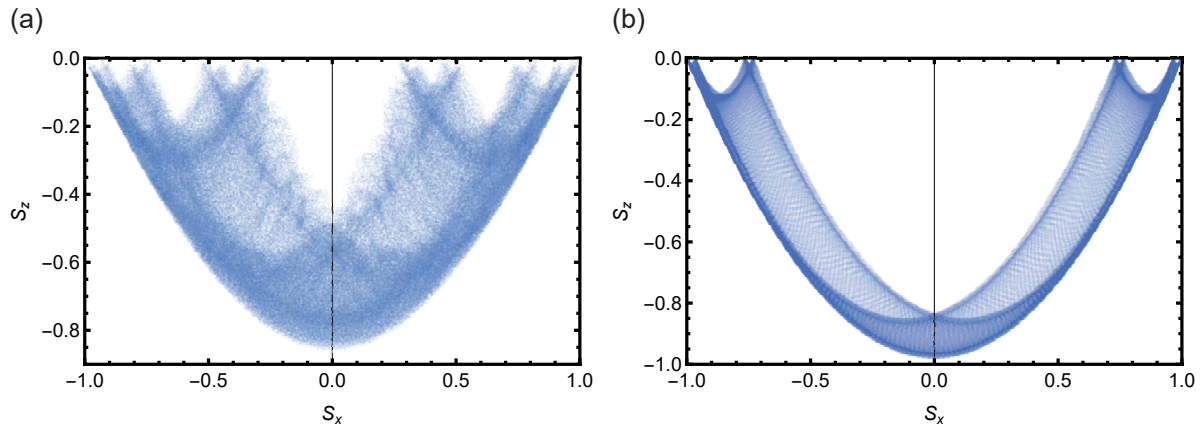


**Figure 2.** Graphs that consist of dots of  $\mathcal{S}(t)$  for the two-photon JCM ( $l = 2$ ). (a)  $\beta = 1.0$ . (b)  $\beta = 2.0$ .

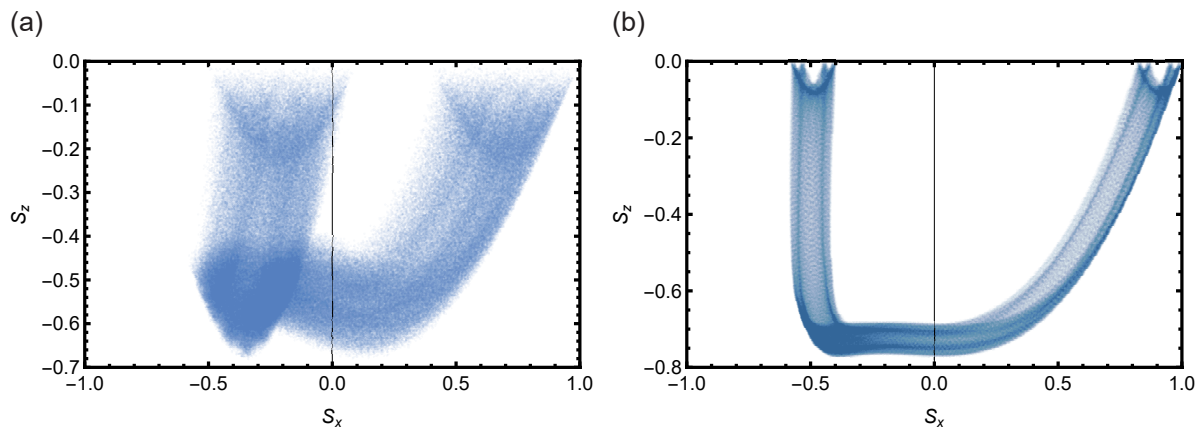


**Figure 3.** Graphs that consist of dots of  $\mathcal{S}(t)$  for the three-photon JCM ( $l = 3$ ). (a)  $\beta = 0.6$ . (b)  $\beta = 1.2$ .

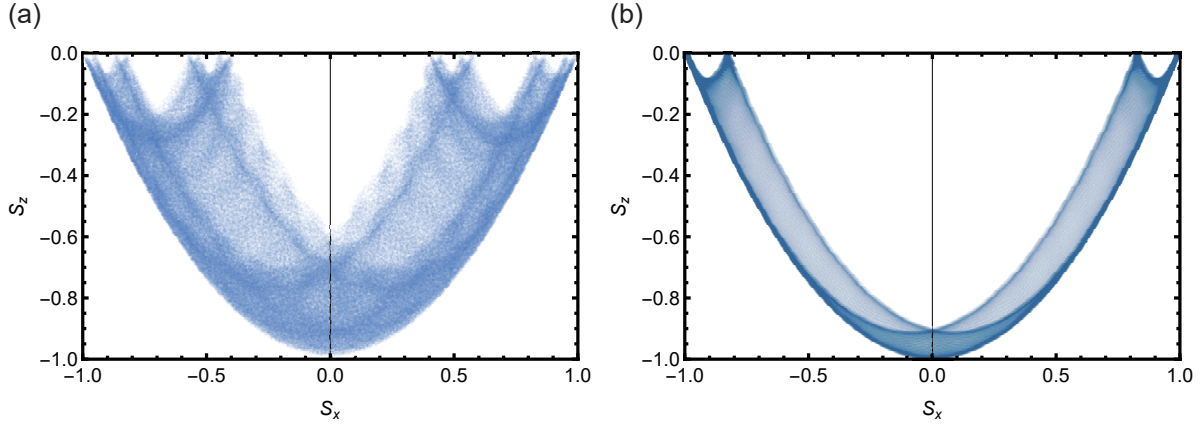


**Figure 4.** Graphs that consist of dots of  $\mathbf{S}(t)$  for the four-photon JCM ( $l = 4$ ). (a)  $\beta = 1.2$ . (b)  $\beta = 2.4$ .

$m\Delta t \pmod{2\pi} \neq 0 \forall m$  holds and  $\mathcal{S}_N$  becomes a uniformly distributed set. Second, we assume  $\pi < \Delta t \pmod{2\pi}$ . Then, whenever the number of the sequence progresses from  $n\Delta t$  to  $(n+2)\Delta t$ , the congruence of modulo  $2\pi$  occurs certainly. Thus,  $(x_0, x_1, x_2, \dots, x_N)$  becomes a pseudorandom sequence according to the method of the linear congruential generator.

From the above, we can regard  $(0, \Delta t, 2\Delta t, \dots, N\Delta t)$  as a pseudorandom sequence uniformly distributed in the range  $[0, 2\pi)$ . The components of  $\mathbf{S}(t)$ , that is to say,  $L^{(1)}(t)$  and  $L^{(4)}(t)$ , depend on  $t$  via terms of  $\cos(\sqrt{D_n}t)$ ,  $\cos(\sqrt{D'_n}t)$ , and  $\sin(\sqrt{D_n}t)$  where

$$D_n = \prod_{k=1}^l (n+k), \quad (22)$$

$$D'_n = \begin{cases} \prod_{k=1}^l (n-k+1) & \text{for } n \geq l, \\ 0 & \text{for } n \leq l-1, \end{cases} \quad (23)$$

with  $\omega = 1$ ,  $g = 1$ , and  $\Delta\omega = 0$ . Further,  $\sqrt{D_n}$  and  $\sqrt{D'_n}$  must be real, positive, but not transcendental. Thus, we cannot distinguish the graph that consists of  $(L^{(1)}(t), L^{(4)}(t))$  for  $t \in \mathcal{S}_N = \{n\Delta t : n = 0, 1, \dots, N\}$  from the graph that consists of  $(L^{(1)}(t'), L^{(4)}(t'))$  for  $t' \in \mathcal{S}'_N = \{n\Delta t' : n = 0, 1, \dots, N\}$  with  $\Delta t' = s\Delta t$  in the limit of  $N \rightarrow +\infty$ . Hence, we can conclude that the graph of  $\{(L^{(1)}(t), L^{(4)}(t)) : t = n\Delta t, n \in \{0, 1, \dots, N\}\}$  is invariant under the scale transformation  $\Delta t \rightarrow s\Delta t$  for  $\pi < s\Delta t \pmod{2\pi}$  with  $\pi < \Delta t \pmod{2\pi}$ .

#### 4. Derivation of the time $t$ for $|S_z(t)| \ll 1$ with the Diophantine approximation

In Fig. 5, we plot  $S_x(t_n)$  with red points as a function of  $\beta$  for the discrete-time values  $t_n = n\Delta t$  where  $|S_z(t_n)| < \epsilon$  holds for a small positive number  $0 < \epsilon \ll 1$  with  $l = 1, 2, 3, 4$ , respectively.

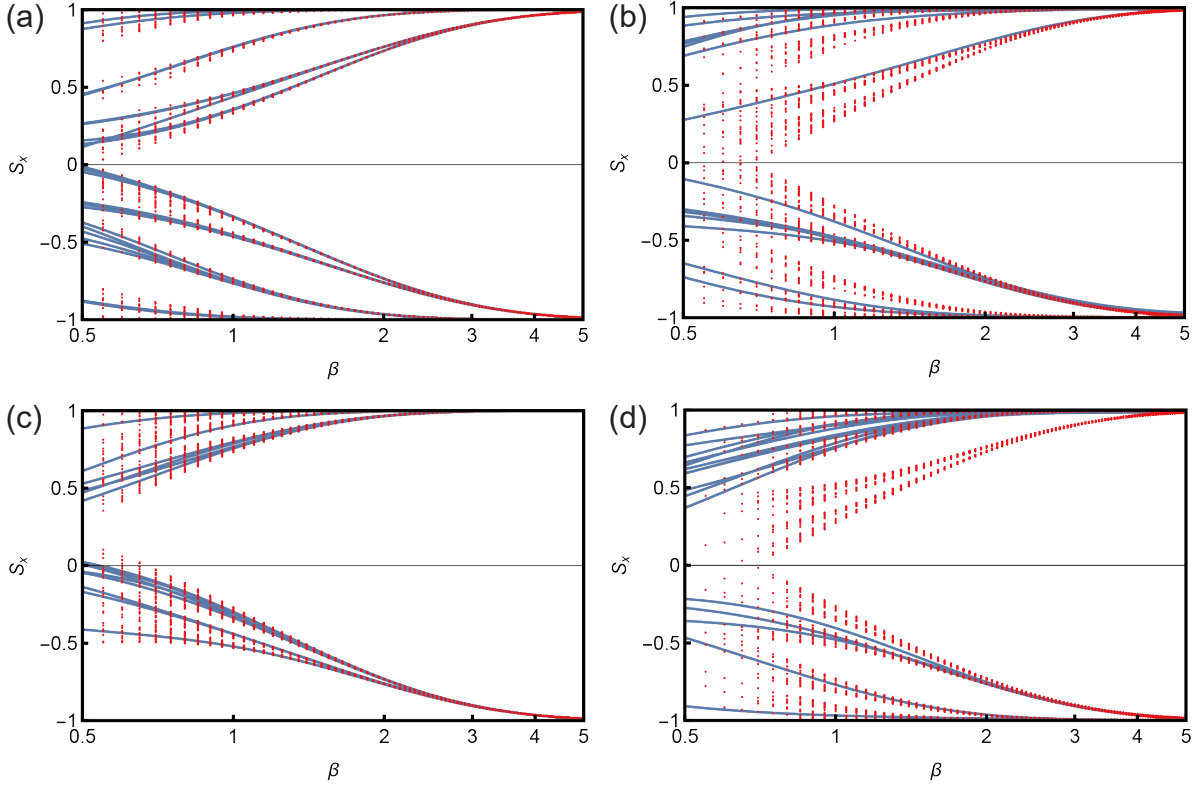


**Figure 5.** Red points represent  $(\beta, S_x(t_n))$  for  $t_n = n\Delta t$  where  $|S_z(t_n)| < \epsilon$  with a small positive number  $\epsilon$  ( $0 < \epsilon \ll 1$ ). Calculating  $S_x(t_n)$  and  $S_z(t_n)$ , we set parameters as  $\Delta t = 4$ ,  $g = 1$ ,  $\omega = 1$ , and  $\Delta\omega = 0$ . The horizontal axis is shown with the logarithmic scale. For  $2 \leq \beta \leq 5.0$ , we set  $\epsilon = \epsilon_0$ . By contrast, for  $0.5 \leq \beta < 2.0$ , we put  $\epsilon = \epsilon_0 \exp[c_0(2.0 - \beta)]$ . Selecting  $t_n$  that satisfies  $|S_z(t_n)| < \epsilon$ , we try  $t_n = n\Delta t$  for  $n = 0, 1, \dots, N$  where  $N$  is a large number. How to set  $N$  is as follows. For  $0.5 \leq \beta < 1.0$ ,  $1.0 \leq \beta < 2.0$ ,  $2.0 \leq \beta < 3.0$ , and  $3.0 \leq \beta \leq 5.0$ , we put  $N = N_0$ ,  $N = N_0/2$ ,  $N = N_0/5$ ,  $N = N_0/10$  with  $N_0 = 1000000$ , respectively. Blue curves represent  $S_x(t)$  with  $t = q\pi$  and  $q \in \tilde{\mathcal{M}}$  that is given by Eq. (48) and Appendix A. Looking at these graphs, we note that some red points lie on the blue curves. (a)  $l = 1$  (the original JCM),  $\epsilon_0 = 0.0035$ ,  $c_0 = 0.7$ . (b)  $l = 2$  (the two-photon JCM),  $\epsilon_0 = 0.009$ ,  $c_0 = 0.6$ . (c)  $l = 3$  (the three-photon JCM),  $\epsilon_0 = 0.0024$ ,  $c_0 = 1.5$ . (d)  $l = 4$  (the four-photon JCM),  $\epsilon_0 = 0.009$ ,  $c_0 = 0.7$ .

Now, we consider how to derive the value of the time variable  $t$  that satisfies  $|S_z(t)| < \epsilon$  analytically. Assuming  $g = 1$ ,  $\Delta\omega = 0$ , and  $\omega = 1$ , we rewrite  $L^{(4)}(t)$  as

$$L^{(4)}(t) = -\frac{1}{2}(1 - e^{-\beta l})[1 - (1 - e^{-\beta}) \sum_{n=0}^{\infty} e^{-n\beta} \cos(2\sqrt{D_n t})]. \quad (24)$$

Hence,  $L^{(4)}(t) = 0$  holds  $\forall \beta$  if  $\cos(2\sqrt{D_n t}) = 1 \forall n$ .

First, we consider a case where  $n = 0$ . Because  $D_0 = l!$  from Eq. (22), what we must compute is a real value of the time variable  $t$  that satisfies

$$1 - \cos(2\sqrt{l!t}) = \epsilon_0, \quad (25)$$



for a small positive number  $0 < \varepsilon_0 \ll 1$ . Second, we consider a case where  $n = 1$ . Because  $D_1 = (l + 1)!$  from Eq. (22), the time variable  $t$  that we want to compute satisfies

$$1 - \cos(2\sqrt{(l + 1)!}t) = \varepsilon_1, \quad (26)$$

for a small positive number  $0 < \varepsilon_1 \ll 1$ . From Eq. (25), we obtain

$$t \simeq \frac{q}{\sqrt{l!}}\pi \quad \text{for } q = 0, 1, 2, \dots \quad (27)$$

Substituting Eq. (27) into Eq. (26), we obtain

$$\cos(2\sqrt{l + 1}q\pi) \simeq 1 - \varepsilon_1. \quad (28)$$

Thus, we can derive equations,

$$|2\sqrt{l + 1}q\pi - 2p\pi| < \delta(\varepsilon_1) \ll 1, \quad (29)$$

$$|2\sqrt{l + 1}q\pi - 4p\pi| < \delta(\varepsilon_1) \ll 1, \quad (30)$$

$$|2\sqrt{l + 1}q\pi - 6p\pi| < \delta(\varepsilon_1) \ll 1, \quad (31)$$

...

where  $\delta(\varepsilon_1) = |\arccos(1 - \varepsilon_1)|$ .

To let Eqs. (25) and (26) hold, it is all right that only one of Eqs. (29), (30), (31), ... is satisfied for a specific positive integer  $p$  that is coprime with  $q$ . Thus, we must find positive integers  $q$  and  $p$  such that

$$\left| \frac{\sqrt{l + 1}}{k} - \frac{p}{q} \right| < \frac{\delta(\varepsilon_1)}{2kq\pi}, \quad (32)$$

for one of a positive integer  $k = 1, 2, 3, \dots$ . Summarizing the above, we want to find positive integers  $p$  and  $q$  where

$$\left| \frac{\sqrt{l + 1}}{k} - \frac{p}{q} \right| = \frac{1}{cq^{1+\nu}} \quad \text{for } k = 1, 2, 3, \dots, \quad (33)$$

with constant values  $c$  and  $\nu > 1$ .

Here, we introduce the following theorem that relates to the Diophantine approximation [21, 22]. For an arbitrary irrational number  $\alpha$ , there exists infinite sequence  $p_m$  and  $q_m (> 0)$  for  $m \geq 0$  such that  $p_m$  and  $q_m$  are coprime and

$$\left| \alpha - \frac{p_m}{q_m} \right| < \frac{1}{q_m^2}. \quad (34)$$

In general, it is known that computation of first some terms of a continued fraction representation of an irrational number gives us its Diophantine approximation [21, 22]. Describing the continued fraction of an arbitrary irrational number  $\alpha$  as

$$\begin{aligned} \alpha &= a_0 + \frac{1}{a_1 + \frac{1}{a_2 + \frac{1}{\ddots}}} \\ &= [a_0; a_1, a_2, \dots], \end{aligned} \quad (35)$$

where  $a_0$  is an integer and  $a_1, a_2, \dots$  are positive integers, we define infinite sequences of integers  $(p_0, p_1, p_2, \dots)$  and  $(q_0, q_1, q_2, \dots)$  such that

$$\frac{p_m}{q_m} = [a_0; a_1, a_2, \dots, a_m]. \quad (36)$$

Then, the following relationships hold,

$$\left| \alpha - \frac{p_m}{q_m} \right| \leq \frac{1}{a_{m+1} q_m^2} \quad \text{for } m = 0, 1, 2, \dots \quad (37)$$

Now, using the above fact, we compute  $t = q\pi$  that satisfies  $|S_z(t)| \ll 1$  for  $l = 2$ , that is to say, the two-photon JCM. We want to find  $(q_m, p_m)$  for

$$\left| \frac{\sqrt{3}}{k} - \frac{p_m}{q_m} \right| < \frac{1}{q_m^2}. \quad (38)$$

Here, we define the following convenient notation that represents the continued fraction of an irrational number  $\alpha$  as

$$\chi_\alpha(m) = [a_0; a_1, a_2, \dots, a_m] \quad \text{for } \alpha = [a_0; a_1, a_2, a_3, \dots]. \quad (39)$$

Then, we obtain

$$\sqrt{3} = [1; 1, 2, 1, 2, \dots], \quad (40)$$

$$\chi_{\sqrt{3}}(12) = \frac{3691}{2131}, \quad \chi_{\sqrt{3}}(13) = \frac{5042}{2911}, \quad \chi_{\sqrt{3}}(14) = \frac{13775}{7953}, \quad \dots \quad (41)$$

We consider a set of denominators of  $\chi_{\sqrt{3}}(12), \dots, \chi_{\sqrt{3}}(59)$  as

$\mathcal{M}_{\sqrt{3}} = \{2131, 2911, 7953, \dots\}$ . Similarly, we define

$$\begin{aligned} \mathcal{M}_{\sqrt{3}/k} &= \{\text{denominators of } \chi_{\sqrt{3}/k}(12), \dots, \chi_{\sqrt{3}/k}(59)\} \\ &\text{for } k = 2, 3, 4, 5, 6, 7. \end{aligned} \quad (42)$$

Next, we take a union of these sets as

$$\mathcal{M} = \mathcal{M}_{\sqrt{3}} \cup \mathcal{M}_{\sqrt{3}/2} \cup \mathcal{M}_{\sqrt{3}/3} \cup \dots \cup \mathcal{M}_{\sqrt{3}/7} \cup \{0\}. \quad (43)$$

The number of elements of  $\mathcal{M}$  is given by 243. Then, rewriting Eq. (24) as

$$L^{(4)}(t) = -\frac{1}{2}(1-b^l)[1-(1-b)f(t)], \quad (44)$$

$$f(t) = \sum_{n=0}^{\infty} b^n \cos(2\sqrt{D_n}t), \quad (45)$$

$b = e^{-\beta}$  with  $-\epsilon < L^{(4)}(t) < \epsilon$ , we attain

$$-\frac{2\epsilon}{(1-b)(1-b^l)} + \frac{1}{1-b} < f(t). \quad (46)$$

Up to  $O(b^2)$  for  $l = 2$ , we obtain

$$\begin{aligned} &(1-2\epsilon) + (1-2\epsilon)b + (1-4\epsilon)b^2 \\ &< \cos(2\sqrt{D_0}t) + b \cos(2\sqrt{D_1}t) + b^2 \cos(2\sqrt{D_2}t), \end{aligned} \quad (47)$$

where  $D_0 = 2$ ,  $D_1 = 6$ , and  $D_2 = 12$ . The subset of  $\mathcal{M}$  whose element satisfies Eq. (47) with  $\beta = 2.0$  and  $\epsilon = 0.05$  is given by

$$\tilde{\mathcal{M}} = \{0, 15\,731\,042, 1\,117\,014\,753, \dots\}. \quad (48)$$

The number of elements of  $\tilde{\mathcal{M}}$  is equal to 15. Finally, we plot  $(\beta, S_x(t))$  for  $t = q\pi$  and  $q \in \tilde{\mathcal{M}}$  in Fig. 5(b) as blue curves. Looking at Fig. 5(b), we note that the curves correspond to some red points well. However, some other points do not lie on the curves. Thus, we must admit that  $\tilde{\mathcal{M}}$  gives us only part of the whole  $t$  such that  $|S_z(t)| < \epsilon$ . We carry out similar calculations for cases with  $l = 1, 3$ , and 4 and draw curves in Fig. 5(a), (c), and (d). Details of those calculations are described in Appendix A.

## 5. Discussion

In this paper, we study the trajectories of the Bloch vector for the multi-photon JCMs. First, we show that the discrete graphs of them are invariant under scale transformations. Second, we show that we can compute values of the time when the absolute value of the  $z$ -component of the Bloch vector is nearly equal to zero with the Diophantine approximation. The reason why we can observe these phenomena is as follows.

For example, looking at Eq. (24), we note that  $L^{(4)}(t)$  contains the terms  $e^{-n\beta} \cos(2\sqrt{D_n}t)$  for  $n = 0, 1, 2, \dots$ . When we consider the zero-temperature limit,  $\beta \rightarrow \infty$ ,  $e^{-n\beta}$  vanishes for  $n \neq 0$ . However, if the temperature is finite but not equal to zero, we cannot neglect  $e^{-n\beta}$  for  $n \neq 0$  and  $L^{(4)}(t)$  must not be the Fourier series. Similar situation occurs for  $L^{(1)}(t)$ . These properties are the origin of the two results obtained in this paper, that is to say, the scale invariance of Figs. 1, 2, 3, and 4 and the Diophantine approximation appearing in Fig. 5. Hence, the essence of the results of this paper is that the components of the Bloch vector cannot be represented as the Fourier series because of thermal effects.

The scale invariance and the Diophantine approximation are unexpected natures for the multi-photon JCMs according to the knowledge accumulated so far. We think that the original and multi-photon JCMs still have unknown characteristics that should be explored.

## Appendix A. Calculations for obtaining curves drawn in Fig. 5(a), (c), and (d)

In this section, we explain details of how to obtain curves drawn in Fig. 5(a), (c), and (d). For  $l = 1$ , that is to say, the original JCM, we compute the following continued fractions:

$$\sqrt{2} = [1; 2, 2, 2, 2, \dots], \quad (A.1)$$

$$\chi_{\sqrt{2}}(12) = \frac{47\,321}{33\,461}, \quad \chi_{\sqrt{2}}(13) = \frac{114\,243}{80\,782}, \quad \chi_{\sqrt{2}}(14) = \frac{275\,807}{195\,025}, \quad \dots \quad (A.2)$$

We consider a set of denominators of  $\chi_{\sqrt{2}}(12), \dots, \chi_{\sqrt{2}}(39)$  as

$$\mathcal{M}_{\sqrt{2}} = \{33\,461, 80\,782, 195\,025, \dots\}. \quad (\text{A.3})$$

Similarly, we define

$$\begin{aligned} \mathcal{M}_{\sqrt{2}/k} &= \{\text{denominators of } \chi_{\sqrt{2}/k}(12), \dots, \chi_{\sqrt{2}/k}(39)\} \\ &\text{for } k = 2, 3, 4. \end{aligned} \quad (\text{A.4})$$

Then, we take a union of the above sets as

$$\mathcal{M} = \mathcal{M}_{\sqrt{2}} \cup \mathcal{M}_{\sqrt{2}/2} \cup \mathcal{M}_{\sqrt{2}/3} \cup \mathcal{M}_{\sqrt{2}/4} \cup \{0\}, \quad (\text{A.5})$$

where the number of elements of  $\mathcal{M}$  is given by 91. Expanding Eq. (46) up to  $O(b^2)$  for  $l = 1$ , we obtain

$$(1 - 2\epsilon) + (1 - 4\epsilon)b + (1 - 6\epsilon)b^2 < \cos(2t) + b \cos(2\sqrt{2}t) + b^2 \cos(2\sqrt{3}t). \quad (\text{A.6})$$

Taking  $\beta = 2.0$  and  $\epsilon = 0.0035$ , we obtain the subset of  $\mathcal{M}$  whose element satisfies Eq. (A.6) in the form,

$$\tilde{\mathcal{M}} = \{0, 19\,601, 33\,461, 470\,832, \dots\}. \quad (\text{A.7})$$

The number of elements of  $\tilde{\mathcal{M}}$  is equal to 24. Plotting  $(\beta, S_x(t))$  for  $t = q\pi$  and  $q \in \tilde{\mathcal{M}}$ , we draw blue curves in Fig. 5(a).

For  $l = 4$ , that is to say, the four-photon JCM, we compute the following continued fractions:

$$\begin{aligned} \mathcal{M}_{\sqrt{5}/k} &= \{\text{denominators of } \chi_{\sqrt{5}/k}(8), \dots, \chi_{\sqrt{5}/k}(59)\} \\ &\text{for } k = 1, 2, \dots, 8, \end{aligned}$$

$$\mathcal{M}_{\sqrt{5}/9} = \{\text{denominators of } \chi_{\sqrt{5}/9}(8), \dots, \chi_{\sqrt{5}/9}(58)\}, \quad (\text{A.8})$$

$$\mathcal{M} = \mathcal{M}_{\sqrt{5}} \cup \mathcal{M}_{\sqrt{5}/2} \cup \dots \cup \mathcal{M}_{\sqrt{5}/9} \cup \{0\}, \quad (\text{A.9})$$

where the number of elements of  $\mathcal{M}$  is given by 323. (The denominator of  $\chi_{\sqrt{5}/9}(59)$  is too huge so that it is not tractable.) Expanding Eq. (46) up to  $O(b^2)$  for  $l = 4$ , we obtain

$$\begin{aligned} &(1 - 2\epsilon) + (1 - 2\epsilon)b + (1 - 2\epsilon)b^2 \\ &< \cos(2\sqrt{24}t) + b \cos(2\sqrt{120}t) + b^2 \cos(2\sqrt{360}t). \end{aligned} \quad (\text{A.10})$$

Taking  $\beta = 2.0$  and  $\epsilon = 0.04$ , we obtain the subset of  $\mathcal{M}$  whose element satisfies Eq. (A.10) as  $\tilde{\mathcal{M}}$  and its number of elements is equal to 17. We draw the blue curves of Fig. 5(d) with  $\tilde{\mathcal{M}}$ .

For  $l = 3$ , that is to say, the three-photon JCM, the situation is different from the above. Because  $\sqrt{l+1}/k = 2/k$  for Eq. (33), we do not need to compute the Diophantine approximation. Thus, we prepare  $\mathcal{M} = \{0, 1, 2, \dots, 2000\}$  for letting  $q \in \mathcal{M}$  satisfy one of Eqs. (29), (30), (31), .... Expanding Eq. (46) up to  $O(b^2)$  for  $l = 3$ , we obtain

$$\begin{aligned} &(1 - 2\epsilon) + (1 - 2\epsilon)b + (1 - 2\epsilon)b^2 \\ &< \cos(2\sqrt{6}t) + b \cos(2\sqrt{24}t) + b^2 \cos(2\sqrt{60}t). \end{aligned} \quad (\text{A.11})$$

Taking  $\beta = 2.0$  and  $\epsilon = 0.003$ , we obtain the subset of  $\mathcal{M}$  whose element satisfies Eq. (A.11) as  $\tilde{\mathcal{M}}$  and its number of elements is equal to 15. We draw the blue curves of Fig. 5(c) with  $\tilde{\mathcal{M}}$ .

## Acknowledgment

This work was supported by MEXT Quantum Leap Flagship Program Grant No. JPMXS0120351339.

- [1] F. Arute, *et al.* ‘Quantum supremacy using a programmable superconducting processor’, *Nature* **574**, 505 (2019).  
doi:10.1038/s41586-019-1666-5
- [2] A. Osman, J. Simon, A. Bengtsson, S. Kosen, P. Krantz, D. P. Lozano, M. Scigliuzzo, P. Delsing, Jonas Bylander, and A. Fadavi Roudsari, ‘Simplified Josephson-junction fabrication process for reproducibly high-performance superconducting qubits’, *Appl. Phys. Lett.* **118**, 064002 (2021).  
doi:10.1063/5.0037093
- [3] V. Kaushal, B. Lekitsch, A. Stahl, J. Hilder, D. Pijn, C. Schmiegelow, A. Bermudez, M. Müller, F. Schmidt-Kaler, and U. Poschinger, ‘Shuttling-based trapped-ion quantum information processing’, *AVS Quantum Sci.* **2**, 014101 (2020).  
doi:10.1116/1.5126186
- [4] P. Murali, D. M. Debroy, K. R. Brown, and M. Martonosi, ‘Architecting noisy intermediate-scale trapped ion quantum computers’, in *2020 ACM/IEEE 47th Annual International Symposium on Computer Architecture (ISCA)*. IEEE, 2020, pp. 529–542.  
doi:10.1109/ISCA45697.2020.00051
- [5] M. Veldhorst, J. C. C. Hwang, C. H. Yang, A. W. Leenstra, B. de Ronde, J. P. Dehollain, J. T. Muhonen, F. E. Hudson, K. M. Itoh, A. Morello, and A. S. Dzurak, ‘An addressable quantum dot qubit with fault-tolerant control-fidelity’, *Nat. Nanotechnol.* **9**, 981 (2014).  
doi:10.1038/nnano.2014.216
- [6] D. M. Pino, R. S. Souto, and R. Aguado, ‘Minimal Kitaev-transmon qubit based on double quantum dots’, *Phys. Rev. B* **109**, 075101 (2024).  
doi:10.1103/PhysRevB.109.075101
- [7] W.-Q. Liu and H.-R. Wei, ‘Linear optical universal quantum gates with higher success probabilities’, *Adv. Quantum Technol.* **6**, 2300009 (2023).  
doi:10.1002/qute.202300009
- [8] T. Yamazaki, T. Arizono, T. Kobayashi, R. Ikuta, and T. Yamamoto, ‘Linear optical quantum computation with frequency-comb qubits and passive devices’, *Phys. Rev. Lett.* **130**, 200602 (2023); Erratum *Phys. Rev. Lett.* **132**, 109902 (2024).  
doi:10.1103/PhysRevLett.130.200602,  
doi:/10.1103/PhysRevLett.132.109902
- [9] G. Rempe, H. Walther, and N. Klein, ‘Observation of quantum collapse and revival in a one-atom maser’, *Phys. Rev. Lett.* **58**, 353 (1987).  
doi:10.1103/PhysRevLett.58.353
- [10] J. Lee, M. J. Martin, Y.-Y. Jau, T. Keating, I. H. Deutsch, and G. W. Biedermann, ‘Demonstration of the Jaynes-Cummings ladder with Rydberg-dressed atoms’, *Phys. Rev. A* **95**, 041801(R) (2017).  
doi:10.1103/PhysRevA.95.041801
- [11] F. Zou, X.-Y. Zhang, X.-W. Xu, J.-F. Huang, and J.-Q. Liao, ‘Multiphoton blockade in the two-photon Jaynes-Cummings model’, *Phys. Rev. A* **102**, 053710 (2020).  
doi:10.1103/PhysRevA.102.053710
- [12] J. Tang, ‘Quantum switching between nonclassical correlated single photons and two-photon

- bundles in a two-photon Jaynes-Cummings model', *Opt. Express* **31**, 12471 (2023).  
doi:10.1364/OE.487297
- [13] S. Felicetti, D. Z. Rossatto, E. Rico, E. Solano, and P. Forn-Díaz, 'Two-photon quantum Rabi model with superconducting circuits', *Phys. Rev. A* **97**, 013851 (2018).  
doi:10.1103/PhysRevA.97.013851
- [14] R. Puebla, M.-J. Hwang, J. Casanova, and M. B. Plenio, 'Protected ultrastrong coupling regime of the two-photon quantum Rabi model with trapped ions', *Phys. Rev. A* **95**, 063844 (2017).  
doi:10.1103/PhysRevA.95.063844
- [15] P. Laha, P. A. A. Yasir, and P. van Loock, 'Genuine non-Gaussian entanglement of light and quantum coherence for an atom from noisy multiphoton spin-boson interactions', preprint arXiv:2403.10207.
- [16] P. Laha, P. A. A. Yasir, P. van Loock, 'Tripartite multiphoton Jaynes-Cummings model: analytical solution and Wigner nonclassicalities', preprint arXiv:2404.13658.
- [17] H. Azuma and M. Ban, 'Quasiperiodicity in time evolution of the Bloch vector under the thermal Jaynes-Cummings model', *Physica D* **280-281**, 22 (2014).  
doi:10.1016/j.physd.2014.04.009
- [18] H. Weyl, 'Über die Gleichverteilung von Zahlen mod. Eins', *Math. Ann.* **77**, 313 (1916).  
doi:10.1007/BF01475864
- [19] H. Davenport, P. Erdős, W. J. LeVeque, 'On Weyl's criterion for uniform distribution', *Michigan Math. J.* **10**, 311 (1963).  
doi:10.1307/mmj/1028998917
- [20] L. Kuipers, H. Niederreiter, *Uniform Distribution of Sequences* (John Wiley & Sons, Inc., New York, 1974).
- [21] W. A. Coppel, *Number Theory: An Introduction to Mathematics*, 2nd ed. (Springer, Dordrecht, 2009).
- [22] I. Niven, H. S. Zuckerman, *An Introduction to the Theory of Numbers* (John Wiley & Sons, Inc., New York, 1960).